Climate response to tropical cyclone-induced ocean mixing in an Earth system model of intermediate complexity

Sriver, Ryan L.[1,2], Goes, Marlos [3], Mann, Michael E. [1,2], and Keller, Klaus[2,3]

[1] Department of Meteorology, Pennsylvania State University, University Park, PA 16802, USA

[2] Earth and Environmental Systems Institute, Pennsylvania State University, University Park, PA 16802, USA

[3] Department of Geosciences, Pennsylvania State University, University Park, PA 16802, USA

Revised Draft

April 1, 2010

1. Abstract

We introduce a parameterization of ocean mixing by tropical cyclones (TCs) into an Earth system model of intermediate complexity. The parameterization is based on previously published global budgets of TC-induced mixing derived from high-resolution satellite measurements of anomalous sea surface temperatures along storm tracks. Recognizing the caveats introduced, for example, by the simplified model structure, we find that the representation of realistic TC-induced mixing substantially alters the equilibrium conditions of (i) the thermal structure of the upper ocean, (ii) the surface energy budget, and (iii) the circulation in the equatorial to subtropical Pacific ocean. These changes result in warmer upwelling regions in the eastern equatorial Pacific and an overall increase in ocean heat content consistent with the recent TC heat pump hypothesis. Spatial variability in the mixing appears to be a key factor in the modeled response. We find no substantial influence of the considered TC-induced mixing on poleward ocean heat transport in the analyzed model. Our results suggest that climate-sensitive feedbacks are plausible, however, the large-scale effect is mainly confined to the subtropical Indo-Pacific region for present-day TC climatology.

2. Introduction

Understanding the role of tropical cyclones (TCs) within the climate system is an active area of research. There is strong evidence linking low frequency variability in TC activity to tropical sea surface temperatures during the past 60 years [*Emanuel*, 2005]. However, the projected response in activity to future warming is less clear [*Emanuel et al.*, 2008; *Knutson et al.*, 2008; *Bender et al.*, 2010; *Sabbatelli et al.*, submitted]. Furthermore, feedbacks may exist which enable TCs to actively contribute to the dynamics of the climate system, rather than passively responding to changes in the large-scale mean state.

Emanuel [2001] proposed that vertical ocean mixing induced by TC winds may be responsible for the majority of the present-day poleward ocean heat transport. In general, TC winds generate near-inertial internal waves which eventually break [*Black and Dickey*, 2008], mixing warm surface water down into the thermocline where it is available to be advected away from the storm regions by the larger scale ocean circulation. *Emanuel* [2001] hypothesized that this oceanic heat convergence is eventually carried poleward by the meridional overturning circulation, estimating the majority of present-day poleward ocean heat transport can be attributed to TC-induced ocean mixing. Several observation-based studies support this hypothesis [*Sriver and Huber*, 2007; *Sriver et al.*, 2008]. However, these studies find estimates of TC-induced oceanic heat convergence, and the heat available to be transported poleward, is more conservative than the original *Emanuel* [2001] estimate (~30% of peak heat transport values at storm latitudes). Nonetheless, if TCs are capable of influencing tropical temperature patterns through feedbacks associated with ocean mixing and transport, then these events may be an important factor for understanding the nature of climate variability.

The amount of wind energy available to mix the ocean depends on the power dissipated at the surface by friction [*Emanuel*, 2005]. The power dissipation is an integrated measure of TC intensity. It represents the convolution of several cyclone characteristics including wind speed, size, duration, and frequency. While much debate currently focuses on understanding and predicting changes in single metrics such as intensity and frequency, integrated quantities such as power dissipation appear to be more important for describing potential impacts of changes in TC activity on climate. Thus, inferring TC-induced impacts on ocean mixing based on any single metric is incomplete, though there is evidence that certain TC characteristics co-vary (e.g. intensity and duration/frequency) [*Sriver and Huber*, 2007b].

Several recent modeling studies have sought to determine the importance of TC-induced ocean mixing on upper ocean properties and transport. Notably, *Korty et al.* [2008] show that including an interactive mixing parameterization, based on TC maximum potential intensity, into an intermediate complexity climate model positively influences poleward heat transport in climate scenarios with increased atmospheric carbon dioxide, suggesting TCs could be an important factor for sustaining warm climates with a small equator to pole temperature gradient. *Jansen and Ferrari* [2009] show that meridional variability in prescribed TC-induced ocean mixing can inhibit poleward ocean heat transport by influencing the subtropical overturning circulation. They find increased heat convergence at the edge of the subtropics associated with enhanced vertical mixing is eventually transported equatorward in the return branch of the subtropical cells, thus limiting the influence of TC-induced mixing on extratropical transport. *Sriver and Huber* [in press] test the sensitivity of an ocean general circulation model to satellite-based global TC surface winds. They find transient, extreme surface wind forcing alters the subtropical overturning, consistent with *Jansen and Ferrari* [2009]. Furthermore, under scenarios with enhanced TC wind forcing, *Sriver and Huber* [in press] find increased oceanic heat convergence in the tropics and warmer temperatures in upwelling regions, resulting in a permanent El Niño-like climate state. These findings support the idea that increased tropical ocean mixing may have contributed to sustaining a permanent El Niño during the Pliocene (3-5 million years ago) [*Brierley et al.*, 2009; *Fedorov et al.*, 2010].

Here we diagnose the impact of TCs on the large-scale state by incorporating a global parameterization of ocean mixing by these events into an Earth System Model of Intermediate Complexity (EMIC). This parameterization is based on TC-induced mixing budgets developed previously from satellite measurements of anomalous sea surface temperature along storm tracks [*Sriver and Huber*, 2007; *Sriver et al.*, 2008]. The mixing parameterization varies horizontally and vertically. Our aim is simply to test the first-order equilibrium response of large-scale model properties to the inclusion of a simplified (yet arguably realistic) representation of the present-day, observation-based climatology of TC-induced mixing. Furthermore, using an intermediate complexity model enables us to perform a suite of long-term simulations to full equilibrium (including the deep ocean), with relatively low computational burden, and to analyze the effects of varying levels of prescribed background mixing in order to ascertain the relative contribution of TCs to other mixing processes not resolved by the model.

Because the adopted EMIC (similar to many other EMICS) does not yet contain a dynamic atmosphere, we do not capture the full extent of possible atmospheric feedbacks using this modeling approach. For example, TC-induced changes in tropical sea surface temperature patterns may have important implications for the large-scale mean atmospheric circulations such as the Hadley [*Sriver and Huber*, in press] and Walker circulations. Furthermore, changes in regional and tropical surface temperature can influence basin-wide TC activity metrics, such as frequency, intensity, and spatial distribution [*Wang et al.*, 2008; *Zhao et al.*, 2009]. Since our TC mixing parameterization is prescribed, we cannot account for feedbacks that can potentially affect overall TC activity, and more importantly the induced ocean mixing. Here we focus primarily on modeling the impacts of realistic TC-induced mixing on the ocean. This approach is useful for testing the first order response of the ocean to spatially-varying vertical mixing from the present-day global TC climatology. We are presently working on incorporating a climate-sensitive component to our mixing parameterization, utilizing a more sophisticated fully-coupled ocean/atmosphere general circulation model, in order to assess impacts on the coupled ocean-atmosphere system.

The paper is organized as follows: section 3 describes the climate model and experimental design, section 4 contains the results and discussion of the model experiment (including effects on thermal structure, surface energy budget, ocean heat content and transport, and circulation dynamics), and section 5 provides a short description of our main conclusions and the implications.

3. Model

We use the University of Victoria Earth System Model (UVic) [*Weaver et al*., 2001] version 2.8, which features a 3 dimensional ocean general circulation model based on the Modular Ocean Model (MOM) version 2 [*Pacanowski*, 1995]. The UVic model includes a simple energy-moisture balance atmosphere model with prescribed, diagnosed winds, as well as thermodynamic/dynamic sea-ice and thermomechanical land-ice components. This version of the model also includes terrestrial vegetation and carbon cycling [*Meissner et al.*, 2003], and ocean biogeochemistry, based on the ecosystem model of *Schmittner et al.* [2005].

The ocean model is coarsely resolved (1.8° latitude x 3.6° longitude and 19 vertical levels) and features several key mixing parameterizations, including the Gent-McWilliams isopycnal mixing parameterization [*Gent and McWilliams*, 1990], diapycnal mixing over rough topography by tidal forcing [*Simmons et al.*, 2004], and increased vertical mixing rates (1 cm^2/s) below 500 meters depth in the Southern Ocean (south of 40°S) [*Schmittner et al.*, 2009]. In addition, the model uses a prescribed background vertical ocean diffusivity (*Kv*) to simulate the effects of sub-grid scale mixing processes not captured by the parameterizations listed above. Recent studies attempt to constrain the uncertainty of *Kv* used in the UVic model [e.g., *Schmittner et al.*, 2009], suggesting values between 0.2 and 0.3 cm^2/s yield best agreement with observed tracer fields. Here we perform an ensemble of simulations that span a range of *Kv* values from 0.1 to 0.5 cm^2/s, in order to examine the relative contribution of *Kv* in combination with the added prescribed vertical mixing by TCs.

The TC ocean mixing parameterization is based on global mixing budgets developed from satellite-based measurements of anomalous surface temperature along storm tracks [*Sriver and Huber*, 2007; *Sriver et al.*, 2008]. While TCs are transient events, we seek to simplify their modeled representation by characterizing the mixing as annualized diffusivities applied in combination with the *Kv* values. Figure 1A shows a map of the TC mixing rates at the surface. The pattern of mixing is spatially variable with the largest values typically occurring in the regions with the most TC activity. The mixing depths also vary, and we derive these values from the estimated changes in annual mixed layer depth shown previously [*Sriver et al.,* 2008]. Because anomalous mixed layer depth represents only a portion of the total depth affected by TC-induced mixing, we apply an idealized correction by multiplying anomalous mixed layer depth values by 3x. This simplistic approach yields mixing length scales on the order of ~100 meters for diffusivities equal to 1 cm^2/s. Maximum mixing depths penetrate to ~250 meters in areas with the largest TC diffusivities. These mixing rates and length scales are similar to recent estimates based on theoretical arguments [*Korty et al.*, 2008] and modeling results testing the sensitivity of upper ocean properties to TC wind forcing [*Sriver and Huber*, in press]. The model is coarsely resolved in the vertical direction, therefore, we linearly interpolate diffusivity in the deepest grid boxes in order to reflect decreased mixing where mixing depths occur between model levels.

We perform an ensemble of 10 model simulations that span a wide range of UVic *Kv* values (0.1, 0.2, 0.3, 0.4, 0.5 cm^2/s). For each *Kv*, we perform 2 simulations corresponding to cases with TC-induced mixing and without. The model simulations are initiated from modern-day climatology and run for 3000 years to approximate equilibrium. In the final 1000 years of the simulation, the ensemble members are run in a carbon-coupled mode, which couples the atmospheric carbon to the land and ocean models. Atmospheric carbon dioxide levels are prescribed to pre-industrial levels throughout the simulations. We do not address transient climate change forced by increasing atmospheric greenhouse gases in this study. The only difference between each pair of runs for a given *Kv* value is the addition of the TC mixing parameterization that is applied to the oceanic vertical mixing budget. This methodology provides a simple, and flexible, global representation of realistic TC mixing rates suitable for diagnosing the first order importance of these events within the current climate. The simulation results and analysis routines are available from the lead author upon request.

4. Results and Discussion

4.1 Upper-Ocean Thermal Response

The addition of TC-induced mixing in the model significantly alters the upper thermal structure of the global ocean (Figure 1B). The largest effect is seen in the Pacific basin. The northwestern Pacific region exhibits pronounced cooling in the areas experiencing the largest amount of TC activity, consistent with the cyclone-induced ocean heat pump mechanism [*Sriver and Huber*, 2007]. The model exhibits warmer near-surface temperatures in the eastern equatorial Pacific region which is mostly devoid of TCs, consistent with recent independent modeling studies [*Jansen and Ferrari*, 2009; *Fedorov et al*, 2010; *Sriver and Huber*, in press]. These upwelling regions are a key component of the subtropical overturning circulation. This shallow meridional overturning consists of poleward surface Ekman transport, sinking at the edge of the subtropical gyres, and equatorward flow of cooler water at depths of ~200 meters

[*McCreary and Lu*, 1994; *Klinger and Marotzke*, 2000]. In the Pacific, the equatorward flow feeds into the Equatorial Undercurrent, where it is eventually upwelled in the eastern equatorial Pacific region. Thus, our results suggest a substantial portion of the heat pumped into the interior ocean in the Pacific basin is carried equatorward by the return branch of the subtropical cells, leading to anomalously warm upwelling regions in the equatorial cold tongue in the eastern Pacific. This feature suggests Pacific TC activity could provide a mechanism for sustaining a permanent El Niño [*Brierley et al.*, 2009; *Fedorov et al.*, 2010] and is consistent with independent model results testing the sensitivity of an ocean general circulation model to TC winds [*Sriver and Huber*, in press].

While we find some influence on near-surface temperature in other regions experiencing TCs such as the North Atlantic (Figure 1B), the magnitude of the anomalous temperature is substantially less than in the Pacific basin. This result indicates that, within the current global climatology, the effects of TC-induced mixing are largely confined to the dynamics of the Pacific ocean.

4.2 Surface Energy Budget

Although UVic does not contain a dynamic atmosphere component, the simplified energy-moisture balance atmosphere model allows us to diagnose the first-order response of the surface energy budget to changes in upper ocean temperatures forced by TC-induced mixing. The anomalous downward surface heat flux over the ocean between an equilibrated case with TC-induced mixing and the corresponding control is displayed in Figure 2A (for background diffusivity Kv=0.2 cm^2/s). The addition of TC-induced mixing has a strong effect on the model's global surface heat budget over the ocean. Generally, TCs cause a net increase in downward surface heat flux in regions where they occur. The most prominent region of increased downward surface heat flux occurs in the northwestern Pacific (Figure 2A), corresponding to the region experiencing the largest amount of TC activity and coolest temperature response (Figure 1). Figure 2A shows decreased downward heat flux in the eastern equatorial Pacific, consistent with the anomalously warm near-surface temperatures in the eastern equatorial Pacific discussed previously (Figure 1B).

Figure 2B represents the zonally integrated downward surface fluxes from Figure 2A. We find increased oceanic heat convergence at latitudes experiencing TCs, which is again consistent with the cyclone-induced heat pump hypothesis. The low latitudes experience decreased downward surface heat flux associated with warmer eastern equatorial temperatures. The ocean-to-atmosphere heat flux in the mid-latitudes is increased (shown by negative downward flux in Figure 2B), representing warmer temperatures at those latitudes caused by increased poleward heat transport associated with TC-induced ocean mixing.

4.3 Ocean Heat Content and Transport

Following *Emanuel's* [2001] hypothesis (discussed in the introduction), ocean heat convergence by TC-induced mixing should be balanced by increased heat transport under equilibrium conditions. Originally, it was presumed this heat transport would be poleward, thus linking TCs to the wind-driven subtropical gyres and the global meridional overturning circulation, which carry heat and mass to high latitudes. While there is evidence of enhanced poleward heat transport, which increases the ocean-to-atmosphere heat flux in the mid-latitudes (Figure 2B), a substantial portion of this heat remains in the tropics, thus lowering ocean heat uptake in the equatorial oceans. The reason for this modeled response is due to the current-day climatology of TC-induced mixing, which occurs primarily in the Pacific basin between 10 and 30 degrees north. As described previously (section 4.1), the subtropical overturning dominates upper ocean transport in these regions. This circulation tends to trap TC-induced ocean heat in the tropics, which warms the eastern boundary upwelling regions. The tropical warming associated with this TC mixing parameterization appears to limit the effectiveness of TCs as a possible tropical thermostat for the present-day climatology (e.g. distribution, strength, and depth of mixing).

We diagnose global impacts on heat distribution and transport by examining the influence of cyclone mixing on upper ocean heat content (Figures 2C and 2D) for the case with background mixing Kv=0.2 cm^2/s. We find a net increase in heat content between 0 and 500 meters depth for much of the tropics, with the largest warming occurring along the eastern Pacific boundaries. Conversely, the Pacific basin exhibits cooling at intermediate depths between 500 and 1500 meters. Near the surface, the positive anomalous heat content in the Atlantic basin is less than for the other regions. However, the spatial distribution is more uniform in the Atlantic compared to the Pacific and Indian basins. Figure 2C depicts increased heat content along the western boundary in the north Atlantic downstream of the largest amount of TC-induced mixing in that region. This suggests the interaction of the subtropical gyre with the TC-induced mixing is responsible for redistributing some heat poleward in the Atlantic ocean In addition, we find the mean barotropic streamfunction to be sensitive to TC-induced mixing in both the Atlantic and Pacific basins, though there is only a slight positive influence on the strength of the global meridional overturning circulation.

The modeled total poleward ocean heat transport scales with *Kv* in the simulations without TC-induced mixing, but it is relatively insensitive to the TC mixing parameterization (Figure 3). TC-induced mixing tends to inhibit poleward heat transport out of the tropics in the northern hemisphere, consistent with previous model results [*Jansen and Ferrari*, 2009]. Subtropical poleward transport is increased in the both hemispheres, which suggests at least some effect of TC-induced mixing on heat transport by the wind-driven subtropical gyres. However, the relative contribution is small compared to the peak poleward fluxes at these latitudes.

As discussed previously, the heat content in the uppermost 500 meters is increased in the Pacific basin for the simulations with TC-induced mixing, especially in the tropical and subtropical latitudes (Figure 2C). However, below 500 meters, we find decreased ocean heat content in the northern hemisphere maximizing in the central equatorial Pacific (Figure 2D). This feature can be understood by analyzing two simulations with idealized scenarios of prescribed TC-induced mixing. In the first simulation, we applied a constant mixing of 1 cm^2/s across the entire tropics (30S to 30N) to a depth of 200 meters. In the second simulation, we applied the zonally averaged diffusivities (and mixing depths) from our observation-derived estimates (Figure 1A), reflecting a simple zonally-invariant representation of TC-induced mixing that preserves meridional variability. Both idealized simulations were performed for a background diffusivity of Kv=0.2 cm^2/s and were carried out identically to the other ensemble members (see Methods for details). These additional test cases allow us to diagnose the mixing characteristic responsible for the altered thermal structure (e.g. spatial variability in the zonal, meridional, and/or vertical directions).

We find that both simulations with idealized mixing result in more uniform warming of the tropics at all levels in the model, as well as increased poleward ocean heat transport and meridional overturning strength. Thus, there is no cooling below 500 meters in the equatorial Pacific. These simulations suggest that the decrease in equatorial Pacific temperature below 500 meters (Figure 2D) in the model is caused by zonal variability in TC-induced mixing. In other words, zonal mixing gradients in the upper 200 meters can potentially impact the thermal structure of the deep ocean. Changes in these gradients associated with variability in TC-induced mixing may affect heat uptake by the ocean, though timescales at which these effects become important are unclear. Additionally, these results suggest that simplified approaches used to simulate TC-induced mixing, such as broadly increasing vertical diffusivity equally across the entire tropics or certain latitude bands, may over-estimate the influence of these events on the large-scale dynamics. More realistic representations that capture the meridional, zonal, and vertical variability of the mixing may be necessary to accurately simulate the climate response, particularly in scenarios where the characteristics of the mixing may change as a function of the climate state.

4.4 Dynamical Impacts

To examine the influence of TC-induced mixing on the dynamics of the equatorial Pacific, we now focus on the upper ocean temperature and velocity for that basin. Figure

4A shows the zonally averaged temperature and meridional velocity for the control run with background diffusivity Kv=0.2 cm^2/s, and Figure 4B displays the difference between the corresponding run with TC-induced mixing and the control shown in 4A. Figure 4B reflects the substantial increase in temperature within the uppermost 500 meters in the tropics and the decreased temperature in the deeper ocean. The meridional structure of the subtropical overturning circulation is apparent in Figure 4A, with poleward transport in the upper-most 100 meters in both hemispheres and the deeper equatorward flow from ~100 to ~300 meters depth. We find a positive response in the strength of this overturning in the northern hemisphere Pacific, where the majority of TC-induced mixing occurs. There is little influence on the circulation strength in the southern hemisphere cell.

Vertical profiles of the zonally averaged anomalous temperature and eastward velocity for all the TC runs are compared to the corresponding controls for the Pacific basin in Figure 5. The temperature response in Figure 5A is consistent with Figure 4B, reflecting the warm anomaly between the surface and ~400 meters depth. We find that the Equatorial Undercurrent is enhanced in the TC runs, along with intensified westward flow beneath 400 meters depth (Figure 5B). It is important to note peak values of the modeled Equatorial Undercurrent are considerably less than observations (15 cm/s compared to ~100 cm/s), which is a typical limitation in coarse-resolution ocean general circulation models.

The vertical profiles (Figure 5) show that the general response in modeled temperature and velocity are relatively insensitive to the choice of Kv, though the magnitude of the effect depends on the magnitude of Kv. The magnitudes of the temperature anomalies are inversely proportional to *Kv*, with an increased upper ocean warm anomaly for lower background mixing values. The response in the strength of the equatorial near-surface currents depends on the magnitude of the *Kv*, however, the westward velocity anomaly below 200 meters does not. This result suggests that the equatorial westward flow at depth is not a result of the overall mixing strength in the tropics, rather it is due to the spatial variability of the mixing in the zonal directions.

We isolate the zonal structure of the equatorial velocity profile in Figure 5 for the case with background diffusivity *Kv*=0.2. The control case (Figure 6A) shows a well-defined EUC with peak flow from the central to eastern Pacific regions. In Figure 6B, we see the influence of TC-induced mixing on the velocity structure. The model exhibits pronounced eastward flow out of the western Pacific at ~200 meters depth, which feeds warmer water into the Equatorial Undercurrent. As a result, the 20 °C isotherm is deepened by ~10 meters in the TC cases. The intensified equatorial undercurrent is accompanied by deeper anomalously westward flow throughout much of the central Pacific that reaches a maximum in the western Pacific, which is caused primarily by the enhanced TC-induced mixing along the western boundary. This mixing may have impacts on the dynamics on the Indo-Pacific warm pool that could affect transport into the Indian Ocean via the Indonesian Throughflow [*Wijffels et al.*, 2008].

In the model, the TC mixing parameterization increases heat transport into the Indian Ocean via the Indonesian Throughflow, while total volume transport through the Indonesian Throughflow is decreased. In the upper 200 meters, volume transport is increased, which carries anomalously warm water from the western Pacific to the Indian Ocean. Below 200 meters, the westward flow is decreased, and temperature gradients between the basins are small. The net effect is a small decrease in the column-integrated volume transport, along with increased heat transport, within the Indonesian Throughflow. Given the resemblance of the modeled thermal structure to El Niño-like conditions, decreased volume transport is consistent with recent observational results that indicate decreased transport during El Niño events [*Tillinger and Gordon*, 2009]. Thus, our findings suggest TC-induced mixing may influence the dynamics of the Indo-Pacific warm pool, contributing to redistributing heat and mass via the Indonesian Throughflow. However, it is not clear yet whether this result is realistic, given the simplified topography of the Indonesian Throughflow contained in the coarse resolution UVic model. Future experiments with higher-resolution ocean models should better elucidate the robustness of this mechanism.

5. Conclusions

We implement a realistic representation of present-day TC-induced ocean mixing in the UVic Earth System Model. We find the thermal structure of the modeled ocean to be sensitive to our parameterization of this process for all considered values of oceanic vertical background mixing. The thermal response results in altered near-surface temperatures and surface fluxes, along with a redistribution of ocean heat by the large-scale circulation. The main dynamical impacts are confined to the Pacific ocean, where the mixing modifies the subtropical overturning circulation. This results in a decreased zonal temperature gradient with cooler temperatures in the western region and warmer temperatures in the eastern equatorial Pacific. This El Niño-like near-surface temperature pattern is maintained by intensified eastward flow of warm water out of the western equatorial-to-subtropical Pacific, ultimately feeding into the Equatorial Undercurrent and upwelling regions in the eastern Pacific.

Our results suggest that TC-induced mixing based on present-day climatology can have dynamical implications for the global ocean, but the impacts are primarily limited in our model to the tropical (and subtropical) latitudes. We find little evidence that TC-induced mixing influences equator-to-pole poleward ocean heat transport or the meridional overturning circulation within the context of the current climatology. However, our findings do support an active role of TCs within climate that is capable of modifying the thermal and dynamical structure of the ocean, and the possibility of impacts on the meridional overturning in the context of climate change cannot be ruled out. Moreover, the spatial variability of this mixing appears to be a key factor in determining the extent of its impact. TC-induced mixing may have important implications for surface fluxes, tropical temperature distributions and circulation patterns in the tropical and subtropical oceans. A better understanding of how climate-induced changes in TC activity (and the associated changes in ocean mixing) could impact ocean properties and dynamics is needed, though it is unclear at what timescales these processes become important—an issue that will be addressed in future work.

Our current results and interpretations are adorned by the caveats introduced by the lack of a dynamic atmosphere component in UVic. We are, for example, unable to address coupling feedbacks such as changes in trade wind forcing caused by large-scale surface temperature anomalies. Because this forcing is important for regulating the strength of the subtropical overturning, potential feedbacks are likely missing. However, the use of flexible intermediate complexity models such as UVic allows us to examine the first order climate response to TC-induced mixing using an ensemble approach, where we can rigorously test various TC mixing scenarios spanning the full parameter space of applicable background ocean mixing values. Future work is needed to address the possibility of climate feedbacks using a fully-coupled ocean-atmosphere general circulation model.

6. Acknowledgements

We thank Andreas Schmittner and Mike Eby for helpful discussion and supplying a portion of the modified model code applicable to this study. R. Sriver's research was supported by the NOAA Climate and Global Change Postdoctoral Fellowship Program, administered by the University Corporation for Atmospheric Research. M. Mann and K. Keller gratefully acknowledge support from the NSF Paleoclimate program (grant number ATM-0902133). The authors acknowledge the use of the NCAR Command Language (NCL) in the data analysis and visualization.

7. References

Bender, M. A., et al. (2010), Modeled impact of anthropogenic warming on the frequency of intense Atlantic hurricanes, *Science*, *327*, 454-458, doi:10.1126/science.1180568.

Black, W. J., and T. D. Dickey (2008), Observations and analyses of upper ocean responses to tropical storms and hurricanes in the vicinity of Bermuda, *J. Geophys. Res.*, *113*, C08009, doi:10.1029/2007JC004358.

Brierley, C. M. et al. (2009), Greatly expanded tropical warm pool and weakened Hadley circulation in the Early Pliocene, *Science*, *323*, doi:10.1126/science.1167625.

Emanuel, K. A. (2001), The contribution of tropical cyclones to the oceans' meridional heat transport. *J. Geophys. Res*., *106*, 14,771-14,782.

Emanuel, K. A. (2005), Increasing destructiveness of tropical cyclones over the past 30 years, *Nature*, *436*, 686-688, doi:10.1038/nature03906.

Emanuel, K. A., R. Sundararajan, and J. Williams (2008), Hurricanes and global warming: Results from downscaling IPCC AR4 simulations, *Bull. Amer. Meteorol. Soc*., *89*, 347-367, doi:10.1175/BAMS-89-3-347.

Fedorov, A. V., C. M. Brierley, and K. Emanuel (2010), Tropical cyclones and permanent El Niño in the early Pliocene epoch, *Nature*, *463*, 1066-1070, doi:10.1038/nature08831.

Gent, P. R., and J. C. McWilliams (1990), Isopycnal mixing on ocean circulation models, *J. Phys. Oceanogr.*, *20*, 150-155.

Jansen, M., and R. Ferrari (2009), The impact of the latitudinal distribution of tropical cyclones on ocean heat transport, *Geophys. Res. Lett.*, L06604, doi:10.1029/2008GL036796.

Klinger, B. A., and J. Marotzke (2000), Meridional heat transport by the subtropical cell, *J. Phys. Oceanogr.*, *30*, 696-705.

Knutson, T. R., J. J. Sirutis, S. T. Garner, G. A. Vecchi, and I. M. Held (2008), Simulated reduction in Atlantic hurricane frequency under twenty-first-century warming conditions, *Nature Geoscience*, doi:10.1038/ngeo202.

Korty, R. L, K. A. Emanuel, and J. R. Scott (2008), Tropical cyclone-induced upper-ocean mixing and climate: Application to equable climates, *J. Clim.*, *21*, 638-654, doi:10.1175/2007JCLI659.1.

Liu, L. L., W. Wang, and R. X. Huang, (2008), The mechanical energy input to the ocean induced by tropical cyclones, *J. Phys. Oceanogr.*, *38*, 1253-1266, doi:10.1175/2007JPO3786.1.

McCreary J. P., and P. Lu (1994), Interaction between the subtropical and equatorial ocean circulations: The subtropical cell, *J. Phys. Oceanogr.*, *24*, 466-497.

Meissner, K. J., A. J. Weaver, H. D. Matthews, and P. M. Cox (2003), The role of land surface dynamics in glacial inception: a study with the UVic Earth System Model, *Clim. Dyn.*, *21*(7-8), 852 515-537.

Pacanowski, R. C. ed. (1995), MOM 2 documentation: Users guide and reference manual, version 1.0. GFDL Ocean Group Technical Report No. 3, Geophysical Fluid Dynamics Laboratory, Princeton, New Jersey.

Sabbatelli, T. A., M. E. Mann, and S. K. Miller (submitted), Semi-empirical projections of future Atlantic tropical cyclone activity. *Clim. Change.*

Schmittner, A., A. Oschlies, X. Giraud, M. Eby, and H. L. Simmons (2005), A global model of the marine ecosystem for long-term simulations: Sensitivity to ocean mixing, buoyancy forcing, particle sinking, and dissolved organic matter cycling, *Glob. Biogeochem. Cycles*, *19(3)*, GB3004, doi: 10.1029/2004GB002283.

Schmittner, A., N. M. Urban, K. Keller, and D. Matthews (2009), Using tracer observations to reduce the uncertainty of ocean diapycnal mixing and climate carbon-cycle projections. *Global Bio. Cycles*, *23*, GB4009, doi:10.1029/2008GB003421.

Simmons, H. L., S. R. Jayne, L. C. St Laurent, and A. J. Weaver (2004), Tidally driven mixing in a numerical model of the ocean general circulation, *Ocean Modelling*, *6*(34), 245-263.

Sriver, R. L., and M. Huber (2007), Observational evidence for an ocean heat pump induced by tropical cyclones, *Nature*, *447*, 577-580, doi:10.1038/nature05785.

Sriver, R. L., and M. Huber (2007b), Reply to comment by R. N. Maue and R. E. Hart on "Low frequency variability in globally integrated tropical cyclone power dissipation", *Geophys. Res. Lett.*, *34*, L11704, doi:10.1029/2007GL029413.

Sriver, R. L., M. Huber, and J. Nusbaumer (2008), Investigating tropical cyclone-climate feedbacks using the TRMM Microwave Imager and the Quick Scatterometer, *Geochem.,Geophys., Geosyst.*, *9*, Q09V11, doi:1029/2007GC001842.

Sriver, R. L., and M. Huber (In Press), Modeled sensitivity of upper thermocline properties to tropical cyclone winds and possible feedbacks on the Hadley circulation, Submitted to *Geophys. Res. Lett.*

Tillinger, D., and A. L. Gordon (2009), Fifty years of the Indonesian Throughflow, *J. Clim.*, *22*, 6342-6355, doi:10.1175/2009JCLI2981.1.

Wang, C., S.-K. Lee, and D. B. Enfield (2008), Climate response to anomalously large and small Atlantic warm pools during the summer, *J. Clim.*, *21*, 2437-2450, doi:10.1175/2007/JCLI2029.1.

Weaver, A. J., et al. (2001), The UVic Earth system climate model: Model description, climatology, and applications to past, present and future climates, *Atmosphere-Ocean*, *39(4)*, 361-428.

Wijffels, S. E., G. Meyers, and J. S. Godfrey (2008), A 20-yr average of the Indonesian Througflow: Regional currents and interbasin exchange, *J. Phys. Oceanogr.*, *38*, doi:10.1175/2008JPO3987.1.

Zhao, M., I. M. Held, S.-J. Lin, and G. A. Vecchi (2009), Simulations of global hurricane climatology, interannual variability, and response to global warming using a 50-km resolution GCM, *J. Clim.*, *22*, 6653-6678, doi:10.1175/2009JCLI3049.1.

8. Figure Captions

Figure 1. A. Surface map of tropical cyclone diffusivity used as input for UVic climate model simulations. Diffusivities are derived from satellite-based climatology developed in *Sriver et al.* [2008]. **B.** Upper ocean temperature difference between the equilibrium tropical cyclone simulation and the corresponding control for a background diffusivity Kv=0.2 cm^2/s. Difference is averaged over the uppermost 80 meters.

Figure 2. A. Difference in the total downward surface heat flux between the equilibrium tropical cyclone simulation and the corresponding control for background diffusivity Kv=0.2 cm^2/s. Units are Watts/meter^2. **B.** Zonal integration of the heat flux difference shown in Figure 2A. Units are Watts/meter divided by 10^8. **C.** Difference in ocean heat content, integrated from the surface to 500 meters depth, between the equilibrium tropical cyclone simulation and the corresponding control for background diffusivity Kv=0.2 cm^2/s. Units are Joules/meter^2 divided by 10^9. **D.** As in Figure 2C but integrated from 500 meters to 1500 meters depth.

Figure 3. A. Total northward ocean heat transport for control cases with varying background mixing (Kv). Units are in Petawatts (1 Petawatt = 10^{15} Watts). **B.** Difference between cases with TC mixing parameterization and the corresponding control for each Kv.

Figure 4. A. Zonally-averaged potential temperature (color contours) in the Pacific basin for the control case with background diffusivity Kv=0.2 cm^2/s. Black contours represent

the zonally-averaged meridional velocity for the same region (solid – northward, dashed – southward). Meridional velocity contour spacing is 0.5 centimeters/second. **B.** As in Figure 4A but for the difference between the tropical cyclone case and the control. Meridional velocity contour spacing is 0.05 centimeters/second.

Figure 5 A. Vertical profile of the zonally-averaged equatorial potential temperature difference in the Pacific basin. Each curve represents the difference between the tropical cyclone case and the corresponding control for the full range of background diffusivities. **B.** As in Figure 5A but for eastward velocity.

Figure 6. A. Equatorial transect of eastward velocity (color contours) in the Pacific basin for the control case with background diffusivity K_v=0.2 cm^2/s. Black contours represent surfaces of constant temperature for the same region. Temperature contour spacing is 2 °C. **B.** As in Figure 6A but for the difference between the corresponding tropical cyclone case and the control (color contours). The black contours denote the 20 °C isotherm for the tropical cyclone case (dashed contour) and the control (solid contour).

Figure 1

A.

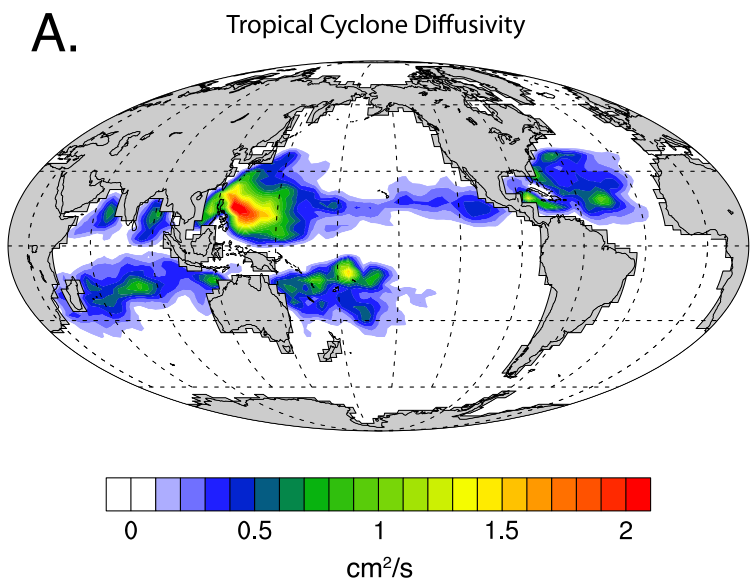
Tropical Cyclone Diffusivity
0
0.5
1
1.5
2
cm²/s

B.

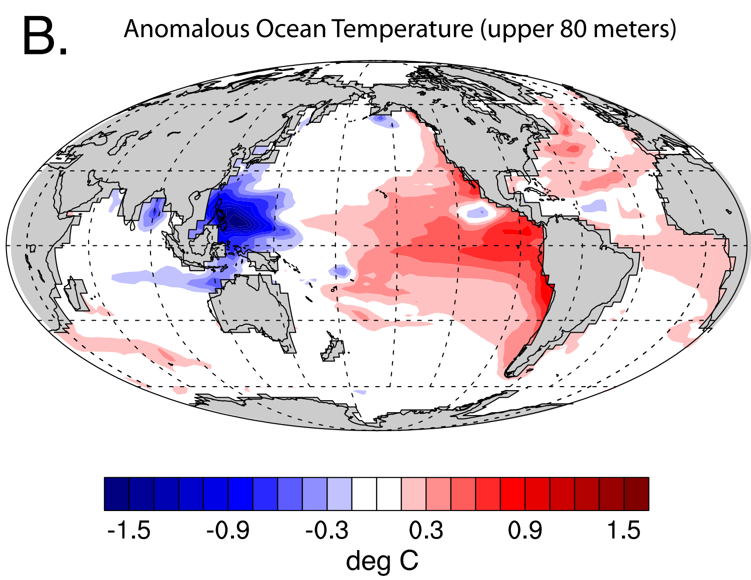
Anomalous Ocean Temperature (upper 80 meters)
-1.5
-0.9
-0.3
0.3
0.9
1.5
deg C

Figure 2

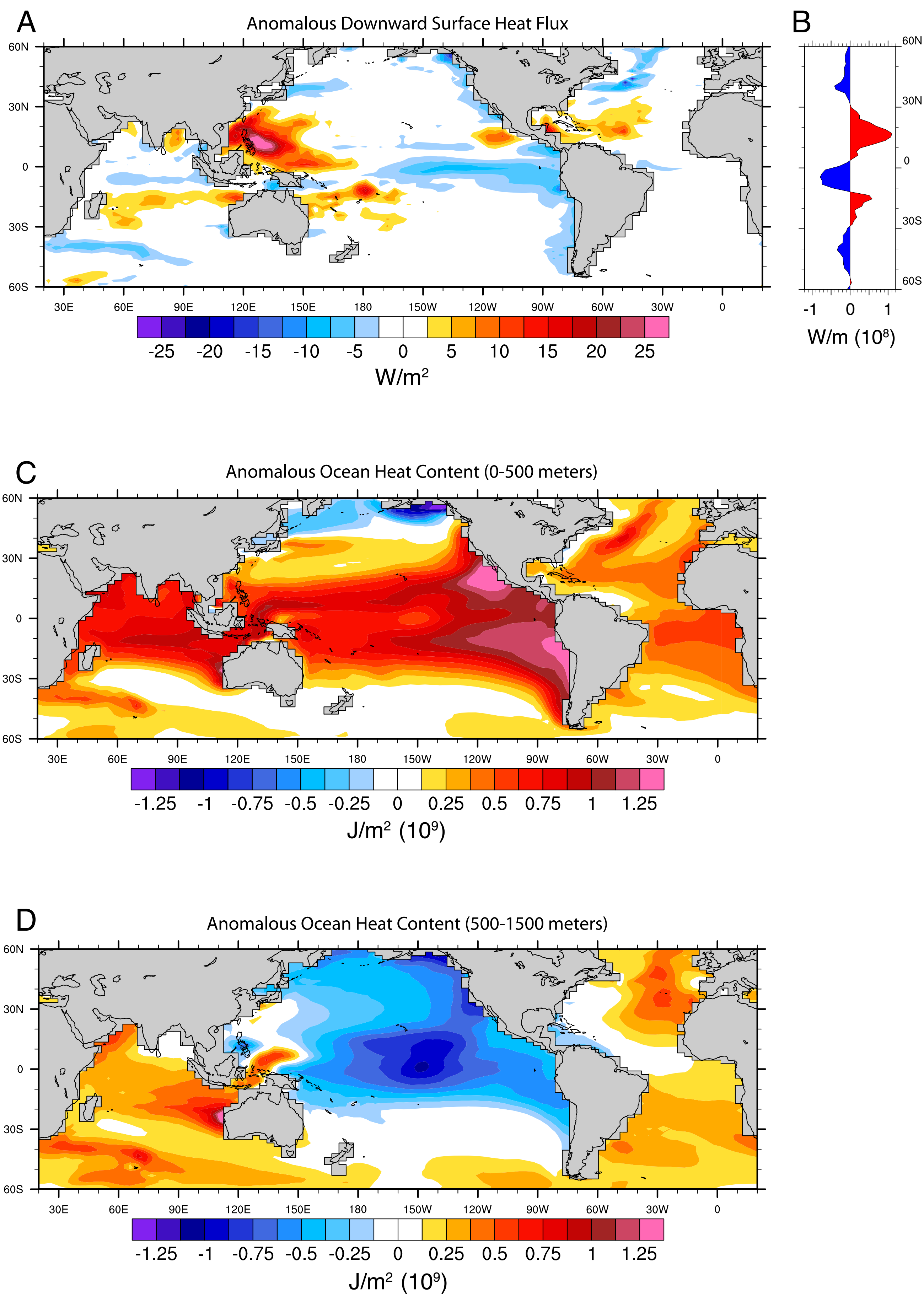
A
Anomalous Downward Surface Heat Flux
60N
30N
0
30S
60S
30E
60E
90E
120E
150E
180
150W
120W
90W
60W
30W
0
-25
-20
-15
-10
-5
0
5
10
15
20
25
W/m²
B
60N
30N
0
30S
60S
-1
0
1
W/m (10⁸)
C
Anomalous Ocean Heat Content (0-500 meters)
-1.25
-1
-0.75
-0.5
-0.25
0
0.25
0.5
0.75
1
1.25
J/m² (10⁹)
D
Anomalous Ocean Heat Content (500-1500 meters)
J/m² (10⁹)

Figure 3

A.

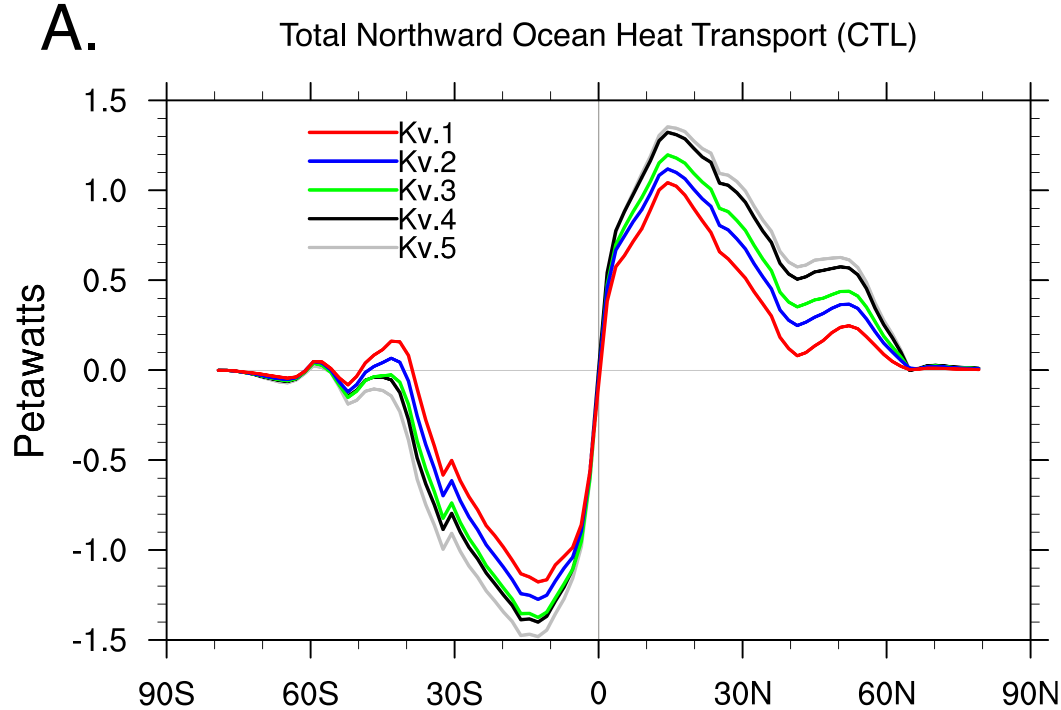
Total Northward Ocean Heat Transport (CTL)
Kv.1
Kv.2
Kv.3
Kv.4
Kv.5
Petawatts
1.5
1.0
0.5
0.0
-0.5
-1.0
-1.5
90S
60S
30S
0
30N
60N
90N

B.

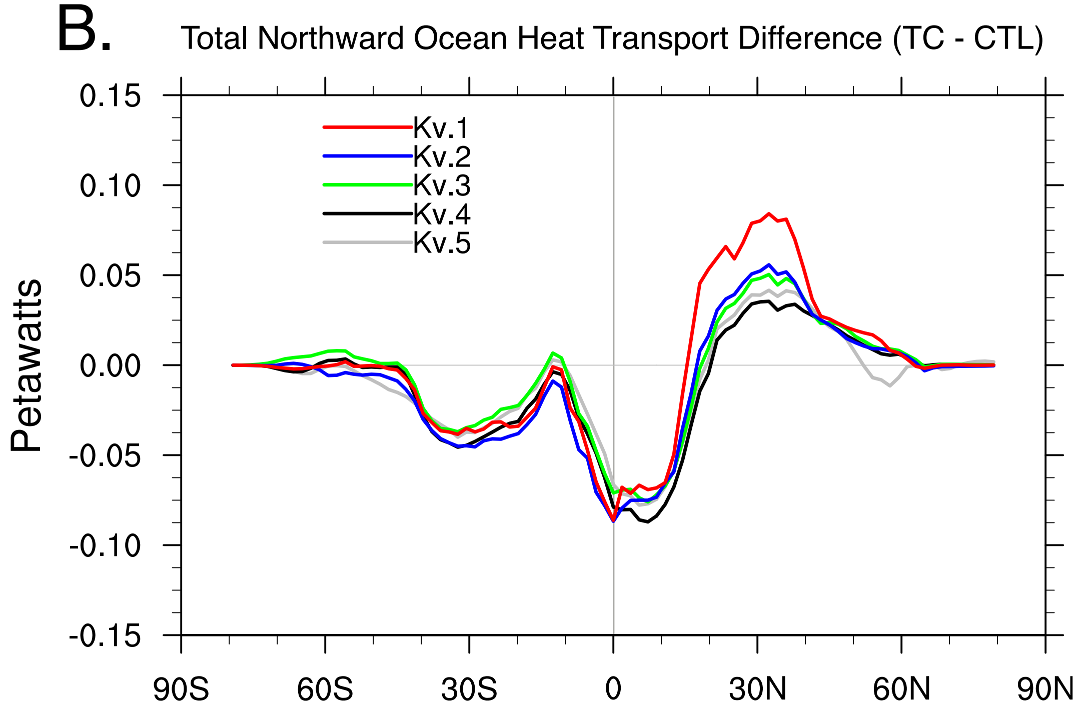
Total Northward Ocean Heat Transport Difference (TC - CTL)
Kv.1
Kv.2
Kv.3
Kv.4
Kv.5
Petawatts
0.15
0.10
0.05
0.00
-0.05
-0.10
-0.15
90S
60S
30S
0
30N
60N
90N

Figure 4

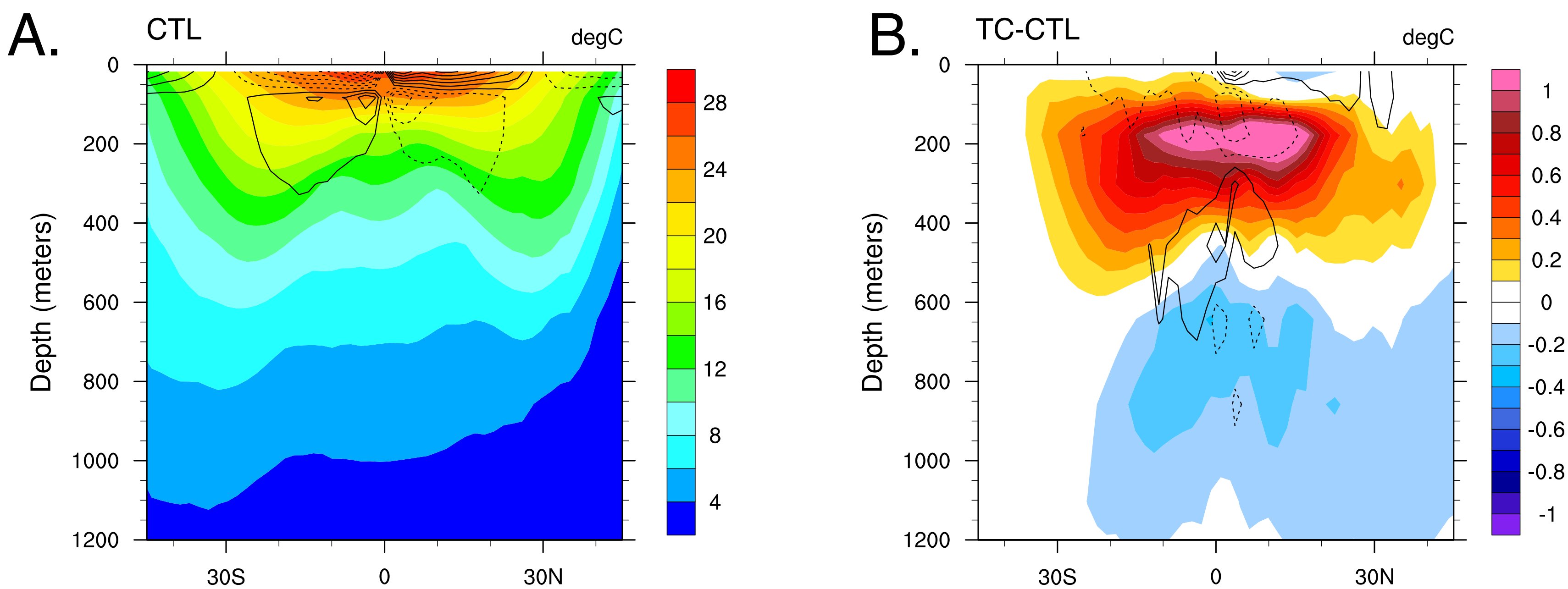
A.
CTL
degC
B.
TC-CTL
degC
Depth (meters)
0
200
400
600
800
1000
1200
30S
0
30N
28
24
20
16
12
8
4
1
0.8
0.6
0.4
0.2
0
-0.2
-0.4
-0.6
-0.8
-1

Figure 5

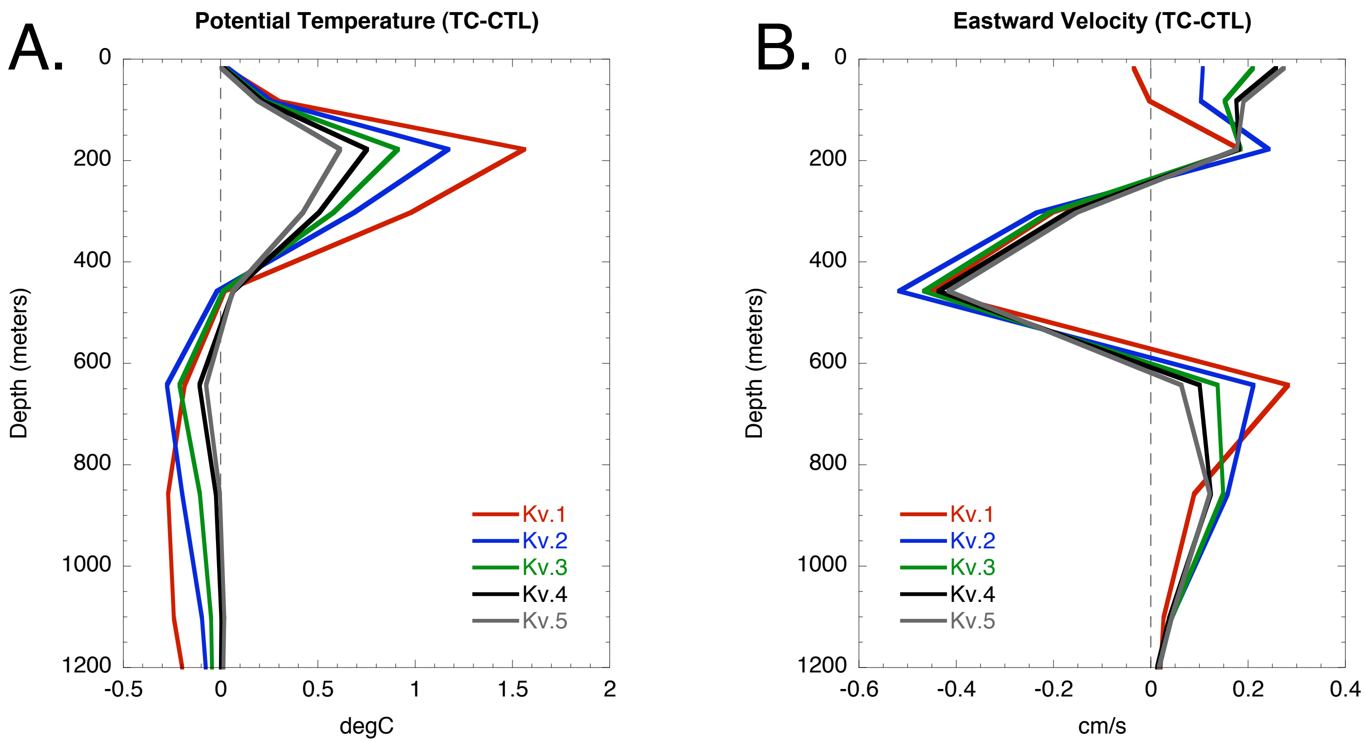
A.
Potential Temperature (TC-CTL)
Depth (meters)
degC
0
200
400
600
800
1000
1200
-0.5
0
0.5
1
1.5
2
Kv.1
Kv.2
Kv.3
Kv.4
Kv.5
B.
Eastward Velocity (TC-CTL)
Depth (meters)
cm/s
-0.6
-0.4
-0.2
0
0.2
0.4
Kv.1
Kv.2
Kv.3
Kv.4
Kv.5

Figure 6

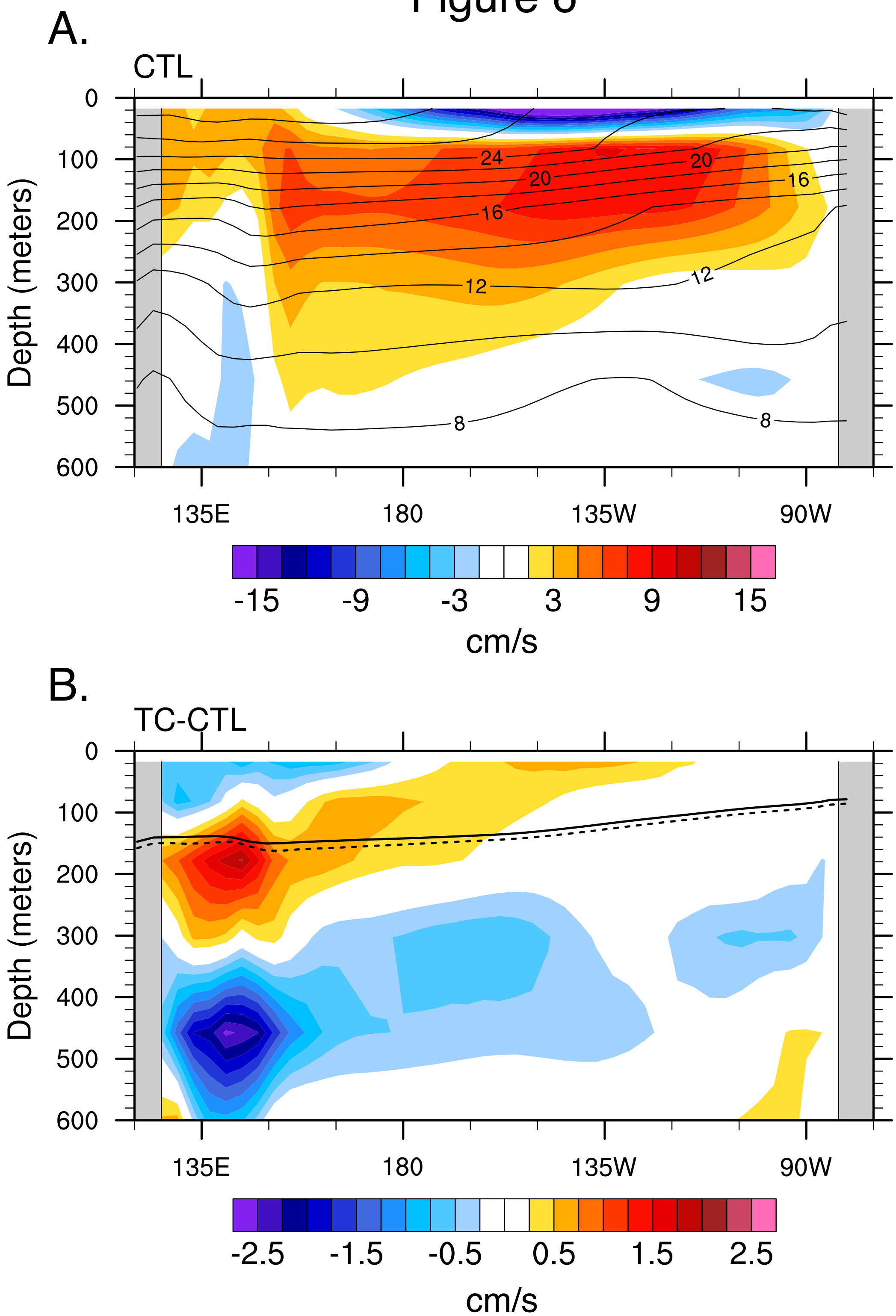
A.
CTL
Depth (meters)
0
100
200
300
400
500
600
24
20
20
16
16
12
12
8
8
135E
180
135W
90W
-15
-9
-3
3
9
15
cm/s
B.
TC-CTL
Depth (meters)
0
100
200
300
400
500
600
135E
180
135W
90W
-2.5
-1.5
-0.5
0.5
1.5
2.5
cm/s